Lunar Module Thermal-Vacuum Simulation Utilizing Conformal Heater Thermal Control

R. HELLMANN,* M. CONOVER,† E. MORRISON,‡ AND G. NEILSON§
Grumman Corporation, Houston, Texas

A Lunar Module Test Vehicle (LTA-8) was placed in a vacuum chamber and subjected to manned thermal-vacuum tests to qualify the LM design for an earth orbital mission. Solar radiation was simulated by the use of conformal skin heaters controlled to predicted heating rates. The heaters consisted of resistance ribbon attached to the skins and controlled by individual power modules. The selection of this solar simulation system was dictated by a combination of vacuum chamber considerations and test requirements. Its features include positive and accurate control of heat input and complete flexibility in achieving various solar simulation postures. Nearly 2000 measurements were utilized to monitor the vehicle structure, subsystems, heaters, vacuum chamber, and astronaut physiological condition. Comprehensive data retrieval and display systems insured successful monitoring and control of the test operation.

Nomenclature

A = area of a surface, ft²
G_s = solar heating rate at earth's orbit, 443 Btu/hr-ft²
Q = heat transferred, Btu; $\dot{Q} = dQ/dt$, Btu/hr
T = temperature, °F
F = geometric view factor; F^* = view factor to the sun, adjusted to include solar radiation reflected from nearby surfaces
$\mathfrak{F}$ = radiant interchange factor between surfaces assumed gray
a = average albedo, applied to a planetary surface
I = electric current applied to a conformal skin heater, amp
R = electrical resistance of a heater, Ω
α = solar absorptance
ϵ = total hemispherical emittance at infrared wavelengths
ϕ = angle locating a flight vehicle from a planetary subsolar point
σ = Stefan-Boltzmann constant, 0.173×10^{-8}, Btu/hr/ft²/°R⁴)

Subscripts

i,j,k = arbitrary vehicle surfaces
f = flight vehicle
n = for heat transfer, from heater skins to vehicle structure
t = thermal-vacuum test vehicle
p = referred to a nearby planet
s,sp = referred to the sun and space, respectively
w = referred to test chamber cold wall

Introduction

THERMAL-VACUUM tests were conducted in May 1968 at the Space Environment Simulation Laboratory, NASA Manned Spacecraft Center, Houston, Texas, to qualify the Apollo Lunar Module (LM) for an earth orbital mission, as successfully flown by Apollo 9/LM-3 in March 1969. This test series included all thermally significant scheduled manned operations as well as exposure to the simulated space environment, and resulted in full acceptance of the basic LM thermal design for earth orbital missions.[1]

Presented as Paper 69-312 at the AIAA 3rd Flight Test, Simulation, and Support Conference, Houston, Texas, March 10–12, 1969; submitted March 18, 1969; revision received September 5, 1969.

* Chief Engineer.
† Data/Programs Group Leader. Member AIAA.
‡ Thermodynamics Project Engineer. Member AIAA.
§ Thermodynamics Engineer.

Configuration

The configuration of the LM is shown by the $\frac{1}{10}$ scale model depicted in Fig. 1. It consists of a descent stage housing primarily the lunar descent propulsion system, landing gear and landing radar, and an ascent stage housing the crew compartment, guidance and navigation systems, environmental control system, ascent propulsion and reaction control systems, and communications and rendezvous radar. The stages are separated for lunar liftoff and the ascent stage alone accomplishes lunar orbital rendezvous with the Apollo command module. The two stages are joined only at four structural supports, an electrical umbilical cable and a fluid line connector block, and are separately insulated.

Insulation of each stage consists of multilayer blankets of aluminized Mylar and polyimide (H-film), covered with protectively coated thermal skins of aluminum and heavy polyimide (Kapton). High-temperature shielding consisting of multilayer nickel and Inconel foil is added locally as required for protection from engine heating and plume impingement.

The LM Vehicle used for this test was basically a production vehicle. It was modified for testing by deactivating all

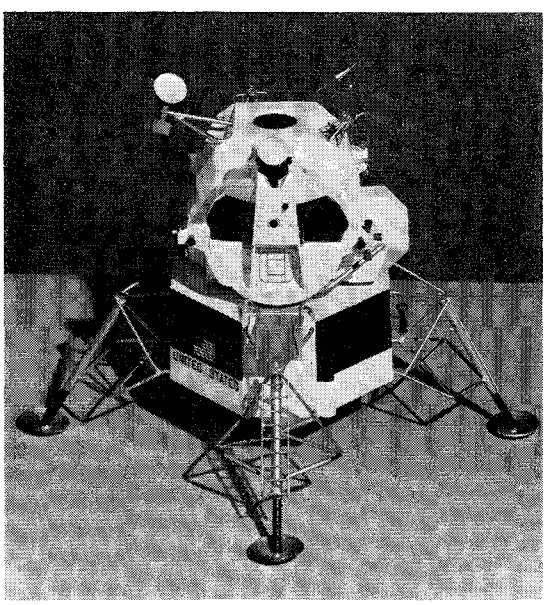

Fig. 1 Model of LM flight vehicle.

Table 1 Characteristics of solar simulation lamps with collimating optics

Advantages	Disadvantages
Resulting temperatures are a direct result of simulated solar heating	Attitude simulation is restricted
Intersurface reflections are accurately reproduced due to the use of collimating optics	Parabolic reflectors do not provide even illumination and heating
No heater cabling is present to block vehicle view of the chamber cold wall (heat sink)	Carbon-arc lamps do not exactly duplicate the solar spectrum
Lamp failures can be repaired during tests (lamps are outside the chamber)	Albedo and planetary radiation can be simulated only crudely by increased "solar" intensity or by auxiliary heaters
Simple, rapid test vehicle/GSE preparation and checkout	Local heating for pretest stabilization and post-test deicing is difficult
The current installation can be used for various test vehicle configurations	Presence of lamp banks reduces area left for the simulated heat sink of black space
	GSE in chamber shadows the vehicle from heating as well as cooling
	Temporary loss of one lamp results in loss of a large fraction of heating

Table 2 Characteristics of heat lamp array around vehicle

Advantages	Disadvantages
Heating from any solar angle and for any vehicle rotation can be simulated, depending on the control mechanism	Special absorptive skin coatings must be used or inputs controlled only to achieve desired skin temperatures
Local application of heating to aid in pretest stabilization and post-test deicing is achievable depending on lamp array geometry	Radiation is not collimated; hence, intersurface reflections are meaningless and perturb test results
Albedo and planetary radiation can be easily simulated	Heating is uneven and difficult to control
Simple, rapid test vehicle/GSE preparation and checkout	Lamp array disturbs vehicle view of chamber cold wall and interferes with access to the vehicle during installation and manned tests
Relatively inexpensive heat lamp installation	Loss of one lamp results in loss of a large fraction of heating with no compensation possible; failures cannot be repaired during tests

propulsion systems, adding instrumentation and conformal heaters. Ground support equipment (GSE) was connected to the vehicle to provide limited systems operation by remote control. Simulators replaced spacecraft batteries during a portion of the test series.

Auxiliary oxygen was made available to the crew in the vehicle for emergency use. Crew communication was conducted via hard lines rather than by antenna radiation. Propellant tanks were filled prior to test, then were detanked as required to simulate expenditure of propellants during simulated engine firings, thus simulating the resulting loss of thermal capacitance.

Thermal-Vacuum Testing

The three thermal tests were characterized as follows. 1) Manrating: demonstration of satisfactory operation of the life support system and all subsystem switching operations, and verification of satisfactory heater operation in a vacuum; and 2) and 3) worst-case cold (hot) mission: a simulated earth orbital mission with coldest (hottest) possible orbital parameters and assuming minimum (maximum) allowable skin absorptances and maximum (minimum) allowable skin emittances.

Prior to each test, after the chamber was pumped down and the cold walls were filled, the vehicle was stabilized to a uniform temperature of approximately 70°F. This closely approximated spacecraft launch conditions, and provided a temperature base for data evaluation. The test timeline was then begun.

The manrating test incorporated several pretest checks of the thermal control system, including: 1) a steady-state vehicle heat balance to determine effective emittance of the insulation system, 2) evaluation and adjustment of heater power levels required for stabilization at 70°F to highlight areas in which adjustment of the thermal analysis was required, and 3) operational checks of all heaters to determine their adequacy for mission simulation and evaluate methods of control.

The mission simulation tests were designed to subject the vehicle to the same thermal conditions as it could experience in accomplishing the earth orbital mission. The timeline included periods of simulated rotation, attitude hold, and entry to and exit from the earth's umbra. These were simulated by varying power applied to the individual conformal heaters. The vehicle was manned and equipment operated as scheduled. Descent and ascent engine heat soakback, RCS engine soakback, and vehicle staging were simulated as scheduled for the flight vehicle. The test ended with crew egress and simulated ascent propulsion system burn to depletion.

Nearly 2000 measurements were used to monitor vehicle and crew conditions in real time. These data were continuously reviewed by the test team in the control room and by subsystem specialists located remotely from the control room.

Solar Heat Simulation System

Selection of conformal skin heaters for LTA-8 testing was based on characteristics of this method of solar heating simulation, on test requirements, and on limitations of the available vacuum chambers. Tables 1, 2, and 3 list the characteristics of three popular methods of solar simulation, any of which

Table 3 Characteristics of conformal skin heaters controlled to predicted heating rates

Advantages	Disadvantages
Heating is very uniform	Skin temperatures result from analytically derived power inputs to the heaters and, therefore, depend on the accuracy of the calculations
Varying solar angles and/or vehicle rotation can be simulated by programing individual heaters	A heater short circuit could damage the skins and/or insulation
Local heating can be biased as required to aid in pretest stabilization and post-test deicing	Heater failures cannot be repaired during tests
Vehicle view of chamber cold wall is not disturbed by the heaters, only by cabling	Test vehicle/GSE preparation and checkout is long and complex
Vehicle skin coatings need only duplicate the long wavelength emittance of the flight coatings	Relatively expensive; each vehicle configuration requires a new set of skin heaters
Loss of one heater affects only a relatively small area and can be partially compensated by increasing the power of adjacent heaters	
Planatary albedo heating can be simulated with the same heaters	

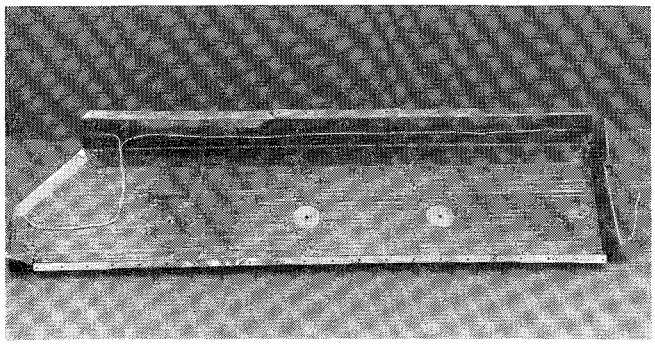

Fig. 2 Conformal ribbon heater installation.

could have been used: 1) carbon-arc lamps with collimating optics, comprising an array of parabolic reflectors lining the chamber wall to flood the vehicle with parallel rays, thus simulating a heat source (the sun) at an infinite distance; 2) local infrared heat lamps arranged immediately around the vehicle, each lamp irradiating a small area of the vehicle; and 3) numerous conformal skin heaters, individually controlled to analytically determined heating rates.

Method 1 offers simplicity of vehicle preparation and use of actual radiation for heat input, at the expense of uneven heating, limitation of available test postures, and a disturbed cold wall heat sink. Method 2 presents problems in both adequacy of simulation and operation, with few compensating advantages. Conformal skin heaters offer excellent control and flexibility of heat input with no limitation in assuming required test postures. Principal disadvantages are complexity of heater installation and checkout and the need to rely on analysis to determine the heat distribution to each skin area.

The test requirement to simulate entire missions accurately and the very long time required for the LM to reach thermal equilibrium made accuracy in simulating skin heating rates critical. The complex external shape of the LM and relatively low solar absorptance made inter-surface reflections important, particularly for the earth orbital LM configuration. Further, because the mission simulated was a near-earth orbital mission, planetary albedo and infrared emission were important.

Only two thermal-vacuum chambers at NASA/MSC are capable of testing a vehicle as large as the LM. Chamber A, the largest man-rated chamber in the Free World, contains a test volume 55 ft in diameter and 90 ft high. It has large collimated carbon-arc solar simulation arrays at one side and the top. The floor is a temperature-controlled turntable, allowing 350° of vehicle rotation about the vertical axis. Chamber B contains a test volume 25 ft in diameter and 30 ft high and has a collimated carbon-arc solar simulation array at the top only.

In summation, direct simulation of solar heating by radiant heating methods cannot satisfy all requirements fully; direct application of energy to the skins through conformal heaters, however, is limited only by the accuracy of the analysis used to determine power distribution. Such heaters had been used successfully in both the Orbital Astronomical Observatory test program and previous LM tests conducted at the Grumman facility in New York. Therefore, taking all factors into consideration, LM testing was scheduled for MSC Chamber B, utilizing conformal heaters.

Thermal Simulation and Control

To permit adequate functioning of the multilayer insulation employed on LM, the pressure must be 1×10^{-5} torr or less. This level was easily achieved in the test chamber through the use of helium-cooled cryopanels spaced around the chamber cold walls, to cryopump oxygen and waste gases from the vehicle. To provide the required black heat sink, the chamber was lined with black, liquid-nitrogen-cooled cold walls. These provided an emittance of greater than 0.90 and an average temperature of approximately 160°R.

Solar heating was simulated by the use of electrical resistance ribbon heaters (called "conformal" heaters because they conform to the shape of the surface to which mounted), applied to the inner surface of all vehicle thermal shield panels and the cabin windows. These skin panels covered every vehicle surface which would be exposed to solar heating at any time during the mission simulated. The conformal ribbon heater installation consisted of a nickel-copper resistance ribbon attached to the skin panel by double-backed, pressure sensitive polyimide tape and electrically insulated from ground by single-backed pressure sensitive polyimide tape (see Fig. 2). The tape had a thermal setting adhesive and served both as a bonding agent and an electrical insulator.

Heat generated by descent, ascent, and RCS engine firings was simulated by the use of sheathed wire heaters attached to the exterior surfaces of the engines. These heaters consisted of Nichrome resistance wire enclosed in a stainless-steel tube, and insulated from it with powdered magnesium oxide. They were attached to the surfaces to be heated by brazing. Woven wire blanket heaters were mounted on the structural backface of the descent stage base heat shield to represent energy radiated and conducted to this large surface during descent engine firings. These heater configurations were chosen to provide high heating rates and to resist high temperatures. They were controlled to follow analytically predicted temperature histories, providing the effect of engine heat soakback to the structure.

Simulation heaters were also installed on power dissipating vehicle components not operated during the test, such as antennas and batteries. The command module simulator was controlled to command module temperatures to simulate the vehicle docked configuration, and cooled to nearly cold wall temperatures to simulate the undocked configuration. This simulator consisted of a slotted disk having the same radiant interchange factors with the upper surfaces of the ascent stage as would the Apollo Command Module (CM) when docked. A temperature-controlled disk at its base simulated the inner surface of the CM docking tunnel. Stabilization ribbon heaters were installed on the propellant and water tanks to assist in the initial stabilization of the vehicle to 70°F. These heaters were not used during testing.

Vehicle heat leaks through the very large number of cables and fluid lines penetrating the insulation and connecting with GSE servicing the vehicle were prevented by insulating and guard heating these penetrations. The design of these guard heaters utilized sheathed resistance wire as used in engine heaters. For cable guard heating, sheathed wires were silver-brazed into heater plate assemblies. The cables were opened and the separate wires spread out in single layers between heater plates and clamped in heavy aluminum frames. For fluid line guard heating, sheathed wires were wrapped and brazed around stainless-steel tubing sections. Multilayer insulation was wrapped around all cables and lines from the vehicle penetrations to the guard heaters, approximately 10 to 40 in.

All guard heaters were controlled to maintain a zero temperature difference with the interior of the vehicle at the fluid line or cable penetration. Each heater utilized a matched pair of platinum resistance temperature sensors, one of which was installed on the guard heater and the other on the vehicle structure. These sensors were connected into a bridge circuit at the guard heater controller, so that a zero bridge unbalance indicated a zero temperature difference. Bridge unbalance served as the input for automatic guard heater control.

Power to all heaters on the test vehicle was supplied by a centralized thermal control system[2] consisting of 480 controlled-current power modules. The output of these modules was manually set by adjusting the variable resistors asso-

ciated with each module. The modules were integrated into three types of control consoles:

1) Ten power control consoles containing 320 power modules used to program power inputs to the conformal skin heaters. Current to the heaters was adjusted as necessary through 10-turn precision potentiometers to supply required power to the heaters.

2) Six temperature control consoles containing 96 power modules and six multiple channel temperature recorders. Current was manually adjusted to control the recorded heater temperatures to predetermined levels.

3) Four guard heater control consoles containing 64 power modules. The differential temperature across each heat flow path was continuously monitored and automatically controlled the power to each guard heater.

To facilitate maintenance, all power modules were physically interchangeable, whether used for power, temperature, or guard heater control, and regardless of load. Switching was used in some cases to enable a module to control either of two heaters not scheduled for use at the same time.

Conformal Skin Heater Power Input Analysis

The LTA-8 thermal characteristics and simulated space environment were designed to correspond as closely as possible to the flight vehicle and its actual space environment; however, two factors were slightly different: 1) emittance of some of the thermal shields and 2) a cold sink temperature of −300°F for the test chamber vs −460°F for space. To compensate for these factors, calculated LM flight vehicle heat inputs required minor modification.

External heat input to the flight vehicle is composed entirely of radiant energy absorption. For any skin panel, this energy consists of direct and vehicle-reflected solar energy, planetary albedo, planetary infrared emission, and infrared emission from adjacent panels. The total heat absorbed by any surface i of the flight vehicle is the sum

gross heat absorbed = solar heat input absorbed + albedo input from nearby planet absorbed + planetary heat input absorbed + heat radiated from adjacent surfaces absorbed; or

$$\dot{Q}_{fi} = (F_{i-s}{}^* + aF_{i-p}\cos\phi)\alpha_i A_i G_s + \sigma A_i \mathfrak{F}_{i-p} T_p{}^4 + \sigma A_i \sum_{j=1}^{k} \mathfrak{F}_{i-j} T_j{}^4 \quad (1)$$

For flight vehicle thermal analysis, direct and reflected solar heating ($F_{i-s}{}^*\alpha_i A_i G_s$) was obtained from a digital computer program which considered diffusely reflecting surfaces and shadowing by intervening surfaces.[3]

Geometric view factors (F) were determined with the aid of a similar program which also considered shadowing by interviewing areas.[4] Finally, evaluation of all radiant interchange factors ($\mathfrak{F}$) was accomplished by a radiosity matrix inversion program.[5] These were the basis of inputs to the vehicle thermal analysis network.

Compensation of the resulting flight vehicle heat inputs to apply to the LTA-8 chamber test is based on equal heat transfer from the skins of both vehicles to the interior structure. Because the skin panels of both vehicles have high ratios of area to thermal capacitance, a steady-state analysis is sufficient.

For surface i of the flight vehicle, a steady-state energy balance is

$$\dot{Q}_{n,f} = (F_{i-s}{}^* + aF_{i-p}\cos\phi)\alpha_i A_i G_s + \sigma A_i \mathfrak{F}_{i-p} T_p{}^4 + \sigma A_i \sum_{j=1}^{k} \mathfrak{F}_{i-j,f} T_j{}^4 - \sigma A_i \left(\mathfrak{F}_{i-p} + \mathfrak{F}_{i-sp} + \sum_{j=1}^{k} \mathfrak{F}_{i-j,f}\right) T_i{}^4 \quad (2)$$

For the corresponding LTA-8 surface,

$$\dot{Q}_{n,t} = I_i{}^2 R_i + \sigma A_i \mathfrak{F}_{i-w} T_w{}^4 + \sigma A_i \sum_{j=1}^{k} \mathfrak{F}_{i-j,t} T_j{}^4 - \sigma A_i \left(\mathfrak{F}_{i-w} + \sum_{j=1}^{k} \mathfrak{F}_{i-j,t}\right) T_i{}^4 \quad (3)$$

For any surface, the sum of all radiant interchange factors applied thereto equals the total hemispherical emittance. Thus,

$$\mathfrak{F}_{j-p} + \mathfrak{F}_{i-sp} + \sum_{j=1}^{k} \mathfrak{F}_{i-j,f} = \epsilon_f \quad (4)$$

and

$$\mathfrak{F}_{i-w} + \sum_{j=1}^{k} \mathfrak{F}_{i-j,t} = \epsilon_t \quad (5)$$

Equating flight and test vehicle expressions for heat transferred to the structure (2) and (3), substituting as in (4) and (5), and solving for electrical power required for the LTA-8 panel, assuming all corresponding skin temperatures equal,

$$I_i{}^2 R_i = (F_{i-s}{}^* + aF_{i-p}\cos\phi)\alpha_i A_i G_s + \sigma A_i \mathfrak{F}_{i-p} T_p{}^4 - \sigma A_i \mathfrak{F}_{i-w} T_w{}^4 + \sigma A_i \sum_{j=1}^{k} (\mathfrak{F}_{i-j,f} - \mathfrak{F}_{i-j,t}) T_j{}^4 - \sigma A_i (\epsilon_f - \epsilon_t) T_i{}^4 \quad (6)$$

Substituting Eq. (1) in (6),

$$I_i{}^2 R_i = \dot{Q}_{fi} - \sigma A_i \sum_{j=1}^{k} \mathfrak{F}_{i-j,t} T_j{}^4 - \sigma A_i \mathfrak{F}_{i-w} T_w{}^4 - \sigma A_i (\epsilon_f - \epsilon_t) T_i{}^4 \quad (7)$$

Equation (7) shows that power required for any surface i consists of that part of the calculated flight vehicle heat input which is supplied externally to the vehicle, less a small corrective term for the infinite cold wall temperature, less a somewhat larger correction, where applicable, for differences in emittance of the test vehicle surface from the corresponding flight vehicle surface.

These corrections were applied to flight vehicle data to arrive at required power levels for each conformal skin heater. Each heater was designed to provide the maximum calculated power with 90% of the rated current of the power module assigned to it, thus providing a margin of power available for rapid temperature adjustments. A computer program was used to select the widest available heater ribbon material possible, to provide 60% to 80% coverage of the back side of each skin panel.[6] Figure (3) shows a model illustrating the distribution of conformal heaters over the LTA-8 vehicle.

Since the flight vehicle continuously varies in angle to the sun, heating rates were calculated for a representative selection of sun angles, and curves of heating rate vs time were compiled for each test vehicle heater. To facilitate manual cycling of the controllers during the test, these curves were approximated by series of step functions having the same total heat input per orbital cycle as the continuous functions.

Conformal Skin Heater Performance

Performance of the conformal skin heaters may be measured in terms of adequacy and accuracy of the thermal simulation, and heater reliability and ability to compensate for heater failure. For adequate thermal simulation, the effect on the vehicle of electrically heating the LTA-8 heater skins must be the same as solar heating of the flight vehicle skins. LTA-8 heater skins were, in some cases, made of thicker sheet stock than flight skins to facilitate heater installation, and were made heavier yet by the mass of heater

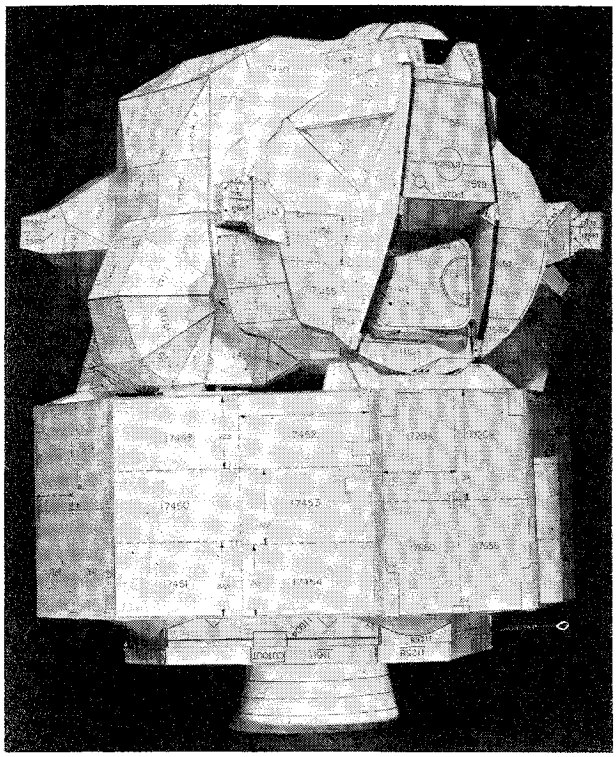

Fig. 3 Nodalized analytical model of the lunar module.

and electrical insulation material. In the worst case, their thermal capacitance exceeded that of the flight vehicle by a factor of 5. This obviously prevented the skins of the LTA-8 vehicle from following the rapid transient temperature changes followed by flight skins. Their design, however, was intended to provide average structural heating rates equal to those of the flight vehicle.

A thermal analysis[7] compared temperature response of LTA-8 heater skins with flight heat shields under the same heat inputs. Figure 4 shows the results for a typical skin panel, showing that, although the LM-3 skins respond faster than LTA-8 skins and experience greater temperature extremes, the average temperature difference from structural temperature is approximately equal, giving equal structural heating. This analysis verifies the adequacy of the conformal heater design to thermally simulate flight vehicle heating.

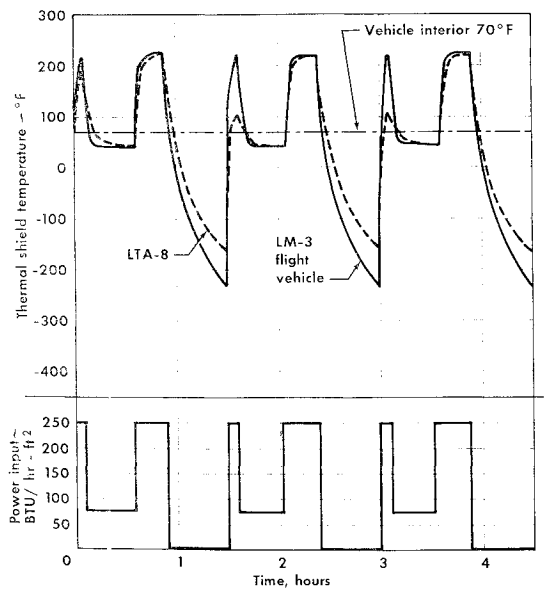

Fig. 4 Analytical temperature response vs power input, LM-3 and LTA-8 thermal shielding for α_s/ϵ = 0.47/0.66.

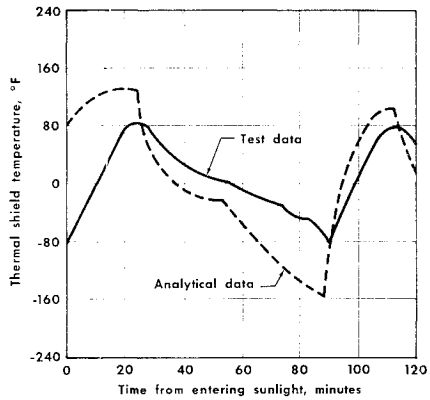

Fig. 5 Ascent stage thermal shield temperature history; typical panel on upper cabin shell.

Comparison of LTA-8 shield temperatures measured during an actual space simulation test with the corresponding analytically predicted shield temperatures shows performance of the heaters as well as quality of the analytical method. This comparison is shown in Fig. 5 for a typical skin panel on the LM ascent stage. The curve of analytical data is for one orbital cycle, and is corrected for in-test deviations. Integration of the curves in Fig. 5 shows that the average temperature of this skin was only 2°F less than the average predicted temperature.

More basically, adequacy of the thermal simulation is shown by the excellent agreement of structural temperatures found in test with predictions. Figure 6 shows average cabin structural temperature as found in test compared with predictions. Test values were within 2°F of analytical predictions except where perturbated by manning, which included equipment operation and operation of the environmental control system (ECS) cooling loop.

Basic reliability of the conformal heater system is attested by the low rate of heater failures. Of the 480 heaters, eleven failed during the man-rating test. These were repaired prior to mission simulation. During the "cold" mission simulation, five heater failures occurred. These could not be repaired before the "cold" test because the tests were run sequentially; thus these five failures were added to five more which failed during the "cold" test.

Compensation for these heater failures was made by dividing the power intended for the failed skin heaters among neighboring heaters. This apportionment was carefully made to avoid overpowering of these heaters.

Data Systems

The focal point of the recording and display system was an Apollo Acceptance Checkout Equipment-Spacecraft (ACE-S/C) Station. This station is a digital system designed to operate on pulse code modulated (PCM) eight-bit data word test data. From LTA-8 within the vacuum chamber, two separate telemetry systems fed subsystem test data to the ACE-S/C. Three instrumentation systems acquired data which were

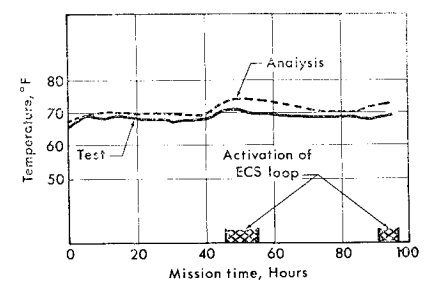

Fig. 6 Average temperature of cabin structure.

Table 4 Measurements per data system

Measurement parameter	PCM telemeter	DFI telemeter	DAA-I	DAA-II	Total
Temperature	35	94	314	817	1260
Pressure	14	5	5	13	37
Flow rate				2	2
Voltage	47	8	4	51	110
Current	11			285	296
Events	91	8	8	2	109
Biomedical			14		14
Energy	2	1			3
Frequency	2				2
rpm	1	4	4		9
Time	1				1
Angles	4			6	10
Quantity	3				3
Total	211	120	349	1176	1856

conditioned and transferred to the interleaver via three 51.2 kilobits per second (kbs) bitstreams: LM PCM Operational Telemeter, Data Acquisition Adapter-Section I, and Data Acquisition Adapter-Section II. In addition, the LM FM/FM Developmental Flight Instrumentation (DFI) telemeters acquired and conditioned test data for recording on magnetic tape for post-test evaluation.

The interleaving device was required to allow almost simultaneous ACE-S/C processing of four 51.2 kbs data bitstreams. Each input bitstream was in synchronization with a master clock (the PCM operational telemeter) and was fed into the interleaver simultaneously. The interleaver then transferred them, serially word-by-word (interleaved), to ACE-S/C at four times the rate of each original bitstream (204.8 kbs). Table 4 shows the distribution of measurements among the data acquisition systems.

The ACE-S/C control room is equipped with 20 active display cathode ray tubes (CRT's). Descriptive annotation and numerical engineering units data were generated by the computer program and arranged on 20 pages of information which was dialed individually for display by any operator. One, two, or three measurements were displayed per line with 24 lines per page. The displayed data was updated once per second.

Four types of ACE-S/C display devices were operated directly from the decommutator rather than the downlink computer; readings from the analog devices (meters and recorders) were displayed in percent of full scale, and event measurements were processed to simultaneously activate an event light and recorder channel. Event and analog recorder strip charts were used in post-test data evaluation.

Since the number of measurements required to control a manned test of this magnitude exceeded the capability of the normal ACE-S/C display devices, a special computer program was developed. The program, upon manual or automatic intervals of five to thirty minutes, sampled 1150 measurements and performed the following computations: 280 measurements, calculate $Q = KI^2R$; 870 measurements, calculate temperatures from nonlinear function.

Immediate computer printouts of these data were transmitted directly to the engineering support room for test evaluation in real time. To provide a calibrated curve for each measurement, a series of X-Y points were fed into the computer program. Operating on these points, the program would "fair" a best-fit fifth-order polynomial through these points utilizing the least-squares method.

All pertinent data concerning each measurement were recorded on magnetic tape in a fixed record format. Three types of magnetic-tape-recorded data were produced by the LTA-8 thermal-vacuum testing activity:

1) Development flight instrumentation—the total output of all DFI measurements.

2) ACE-S/C raw data—the total serial PCM bitstream recorded before entry to the decommutator.

3) ACE-S/C compressed data tape (CDT)—all measurements were subjected to a real-time data processing floating bandpass by the ACE-S/C decommutator and forwarded to the downlink computer for filing on the compressed data tape. This tape permitted analysts to observe trends to a moderately detailed level.

Conclusion

Post-test data analysis indicated that all major test objectives were successfully accomplished. The number of heater control module failures experienced during the test was significant; however, these were expeditiously repaired and returned to their respective control consoles. During repair periods, power to heaters adjacent to those serviced by the failed modules was adjusted to offset the loss of power to the heaters. Conformal skin heater failures were insignificant; therefore, the effects of their loss was easily compensated for in the thermal math model.

References

[1] "90 Day Thermodynamics Report LTA-8/"D" Mission Simulation," Rept. LTR-510-4, Oct. 1968, Grumman Corp.

[2] Myers, G., "Design Control Specification for Thermal Control System," Rept. LSP-410-12050, March 1966, Grumman Corp.

[3] Alaras, J., "A Computer Program to Calculate the Insulation on a System of Planar, Convex, Polygonal Surfaces (Diffuse Reflections)," LTM-(H)-7009-12, Jan. 1965, RCA; also Rept. 72224, Dec. 1965, Grumman Corp.

[4] Alaras, J., "A Computer Program to Calculate Radiative Configuration Factors," LTM-(H)-7009-10, Jan. 1965, RCA; also Rept. 72253, Dec. 1965, Grumman Corp.

[5] Alaras, J., "Computer Program for Evaluating Script F ($\mathcal{F}$) for Radiant Exchange Within an Enclosure," LTM-(H)-7009-9, Feb. 1965, RCA; Repts. 886404, 88450, Dec. 1965, Grumman Corp.

[6] Myers, G., "LTA-8 Heater Design," Rept. LDS 938-1, Vol. I, March 1967 and Vol. IV, July 1968, Grumman Corp.

[7] Chapter, J., "Comparison, Temperature Responses and New Vehicle Heat Loads, LTA-8 and LM-3 Thermal Shield Configurations," Memo LMO-510-714, Dec. 1967, Grumman Corp.